

Supporting Information

Multifunctional luminescent Zn(II)-based metal–organic framework for high proton conductivity and detection of Cr³⁺ ions upon mixed metal ions

Xing Meng,^a Mei-Jie Wei,^b Hai-Ning Wang,^{*a} Hong-Ying Zang^b and Zi-Yan Zhou^{*a}

^aCollege of Chemical Engineering, Shandong University of Technology, Zibo, Shandong, 255049,
P. R. China

^bKey Lab of Polyoxometalate Science of Ministry of Education, Faculty of Chemistry, Northeast
Normal University, Changchun 130024, P. R. China

*Corresponding author

E-mail: wanghn913@foxmail.com; zyzhou@sdut.edu.cn

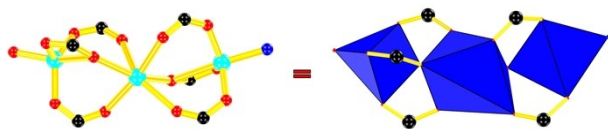


Fig. S1 The trinuclear cluster in compound **1**.

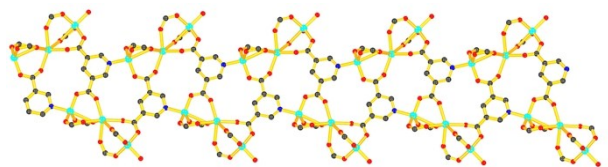


Fig. S2 The two-dimensional sheet structure of the compound **1**.

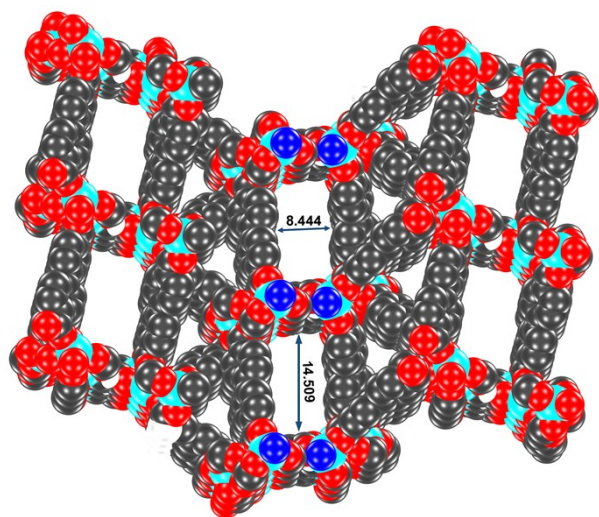


Fig. S3 The three-dimensional framework structure of the compound **1**.

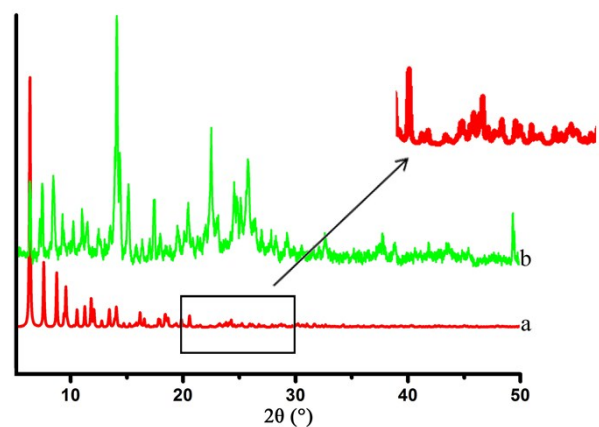


Fig. S4 Powder X-ray diffraction patterns of a) simulated from the X-ray single structure of **1**, b) as-synthesized **1** and an enlarged diffraction patterns corresponding to the area enclosed by the rectangle.

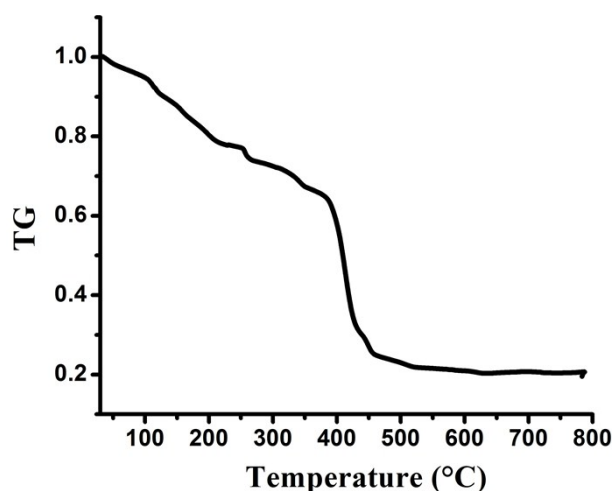


Fig. S5 The TGA curve of compound 1.

Experimental Section

Materials and Measurements. All starting materials and solvents were reagent grade, commercially available and used without further purification. Elemental analyses (C, H and N) were performed on a Perkin-Elmer 2400 CHN elemental analyzer. TG analyses were performed on a HTG-1 Thermogravimetric Analyzer heated from room temperature to 800 °C under air atmosphere at a rate of 5 °C min⁻¹. ICP was measured by Agilent 7500ce.

Synthesis of compound 1: A solution of Zn(NO₃)·6H₂O (0.105 g), 4,4'-Biphenyldicarboxylic acid (0.12 g), 3,5-Pyridinedicarboxylic acid (0.09 g) in DMF (6 mL) was heated at 120 °C for 2 days. The resulting block crystals were collected, washed with ethanol, and dried at room temperature. Elemental analysis for C₅₆H₆₈N₈O₁₉Zn₃ (1353.29) (%): calcd. C 49.70 H 5.06 N 8.28; found C 49.76 H 5.01 N 8.25.

Crystal data for 1: C₅₆H₆₈N₈O₁₉Zn₃, $M_r = 1353.29$, Orthorhombic, space group $P2_12_12_1$. $a = 12.0554(9)$ Å, $b = 14.9560(11)$ Å, $c = 36.898(3)$ Å, $\alpha = 90^\circ$, $\beta = 90^\circ$, $\gamma = 90^\circ$, $V = 6652.7(9)$ Å³, $Z = 4$, $\rho_{\text{calcd}} = 1.351$ g cm⁻³, Reflections collected/unique 24558/6670, $R_{\text{int}} = 0.0920$. The final $R_1 = 0.0488$ ($I > 2\sigma(I)$), $wR_2 = 0.1391$ (all data), CCDC 1571051.

Proton conductivity measurements

The powders were prepared by grinding the sample into a homogeneous powder with a mortar and pestle. The powders were then added to a standard 10 mm die, sandwiched between two stainless steel electrodes and pressed at 15 MPa for 1 min. the pellet was 10 mm in diameter and 0.473 mm in thickness. The impedances were measured with a frequency response analyzer/potentiostat (IviumStat) over a frequency range from 1 Hz to 1 MHz, using a two probe method with Pt-pressed electrodes under an applied ac voltage of 50 mV. The temperature and relative humidity are controlled by using an BPHS-060A incubator. ZSimpWin software was used to extrapolate impedance data results by means of an equivalent circuit simulation to complete the Niquist plot and obtain the resistance values. Conductivity was calculated using the following equation:

$$\sigma = L / RS$$

where σ is the conductivity ($S\ cm^{-1}$), L is the measured sample thickness (cm), S is the electrode area (cm^2) and R is the impedance (Ω).

The powder X-ray diffraction (PXRD) patterns of the prepared sample matches with the simulated data, indicating it possesses high purity (Fig. S4†). The dissimilarities in intensity may be due to the preferred orientation of the crystalline powder samples.

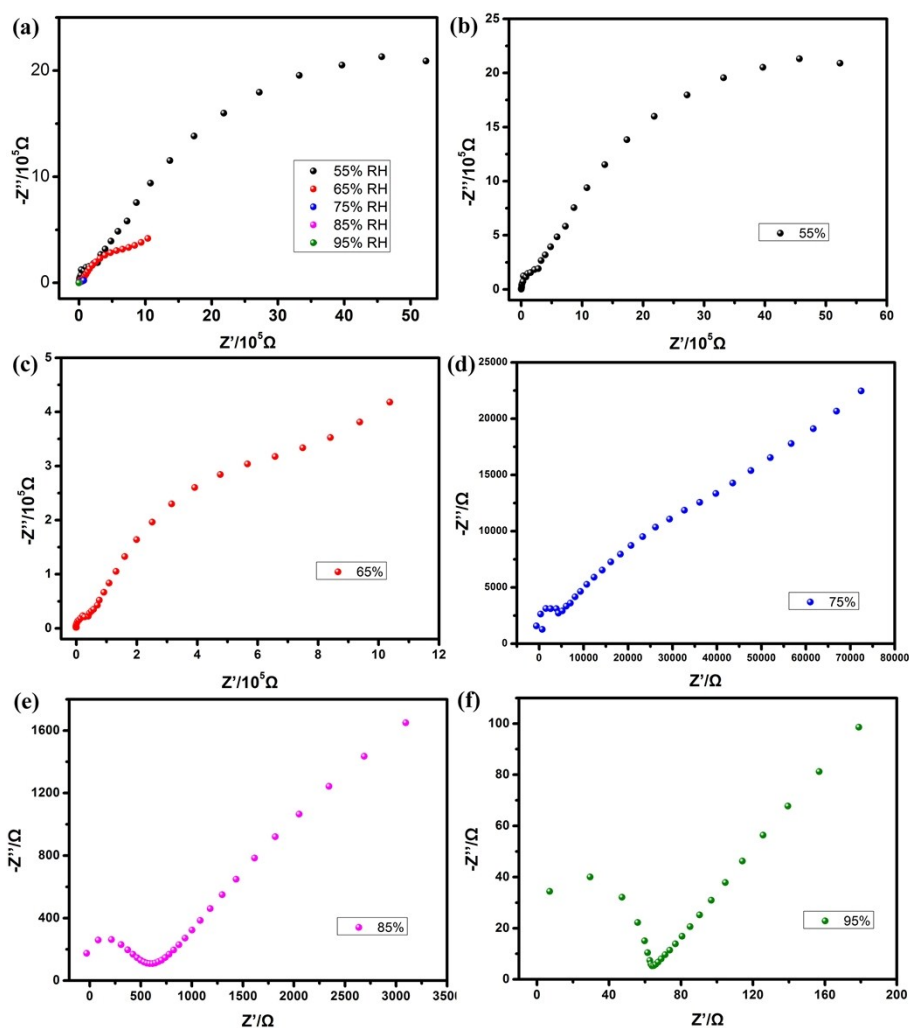


Fig. S6 Impedance spectrum of compound **1** at 25 °C with different RHs.

Table S1 Proton conductivities ($> 10^{-2}$ S cm^{-1}) of selected MOFs.

Compounds	Conductivity (S cm^{-1})	Experimental condition	Ref.
This work	0.95×10^{-2}	60 °C and 97% RH	
Im-Fe-MOF	1.21×10^{-2}	60 °C and 98% RH	1
BUT-83	3.9×10^{-2}	80 °C and 97% RH	2
$\{[\text{Co}_3(\text{m-CIPhIDC})_2(\text{H}_2\text{O})_6] \cdot 2\text{H}_2\text{O}\}_n$	2.89×10^{-2}	100 °C; water and aqua-ammonia vapors ($\text{NH}_3 \cdot \text{H}_2\text{O}$ concentration of 7.40 M)	3
$\{[\text{Co}_3(\text{p-CIPhIDC})_3(\text{H}_2\text{O})_3] \cdot 6\text{H}_2\text{O}\}_n$	4.25×10^{-2}	100 °C; water and aqua-ammonia vapors ($\text{NH}_3 \cdot \text{H}_2\text{O}$ concentration of 7.40 M)	3
UiO-66(-SO ₃ H) ₂	8.4×10^{-2}	80 °C and 90% RH	4
TfOH@MIL-101	8×10^{-2}	60 °C and 15% RH	5
Fe-CAT-5	5×10^{-2}	25 °C and 98% RH	6

$[(\text{Me}_2\text{NH}_2)_3(\text{SO}_4)]_2[\text{Zn}_2(\text{ox})_3]_n$	4.2×10^{-2}	80 °C and 95% RH	7
PCMOF-10	3.55×10^{-2}	70 °C and 95% RH	8
VNU-15	2.90×10^{-2}	95 °C and 60% RH	9
$\text{H}^+@ \text{Ni}_2(\text{dobdc})(\text{H}_2\text{O})_2$ (pH = 1.8)	2.2×10^{-2}	80 °C and 95% RH	10
PCMOF2 _{1/2}	2.1×10^{-2}	85 °C and 90% RH	11
$[\text{ImH}][\text{Cu}(\text{HPO}_4)_{1.5}(\text{HPO}_4)_{0.5} \cdot \text{Cl}_{0.5}]$	2.0×10^{-2}	130 °C and 0 RH	12
HOF-GS-11	1.8×10^{-2}	30 °C and 95% RH	13
$\text{H}_3\text{PO}_4@ \text{MIL-101}$	1.0×10^{-2}	140 °C and 1.1% RH	14
$\text{H}_2\text{SO}_4@ \text{MIL-101}$	1.0×10^{-2}	150 °C and 0.13% RH	14
$\text{CsHSO}_4@ \text{Cr-MIL-101}$	10^{-2}	200 °C and 0 RH	15
$(\text{NH}_4)_2(\text{adp})[\text{Zn}_2(\text{ox})_3] \cdot 3\text{H}_2\text{O}$	10^{-2}	ambient temperature	16

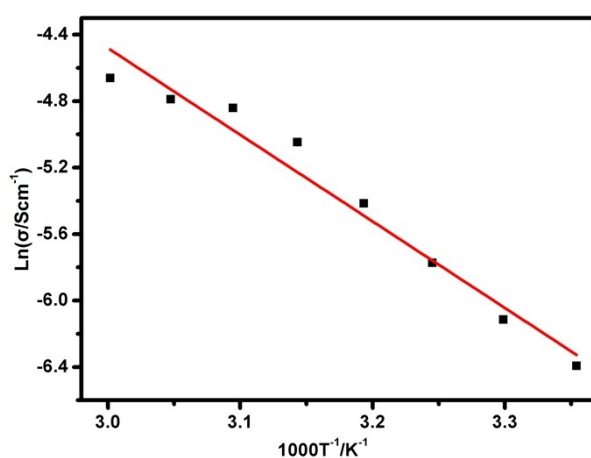


Fig. S7 Arrhenius plot of the proton conductivities of compound 1 at 97% RH.

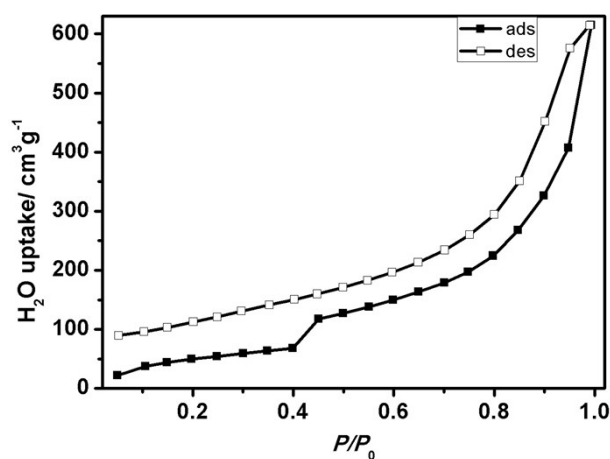


Fig. S8 Water vapor adsorption and desorption isotherms of compound 1 at 25 °C.

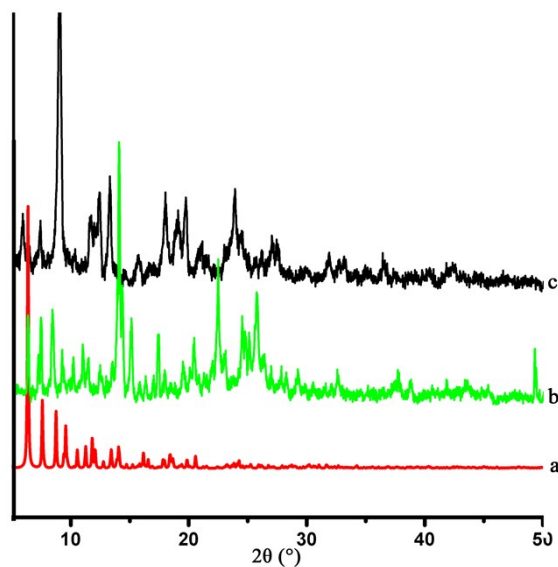


Fig. S9 Powder X-ray diffraction patterns of a) simulated from the X-ray single structure of **1**, b) as-synthesized **1**, and c) after AC impedance measurement.

Luminescent measurements

The luminescence spectra were recorded on a F-380 fluorescence spectrophotometer at room temperature. The strongest emission wavelengths were located at 434 nm when excited at 376 nm. For the experiment of sensing metal ions, the **1**-M^{x+} emulsions were prepared by introducing 3 mg of **1** powder into 5 mL of M(NO₃)_x (M = Zn²⁺, Cu²⁺, Cr³⁺, Cd²⁺, Bi²⁺, Pb²⁺, or Ni²⁺) DMF solution. After sonication treatment 90 min, aging for 1 h, the luminescent spectra were measured. The width of the excitation slit was 2.5 nm and the emission slit was 2.5 nm. In order to determine the amount of Cr³⁺, the inductively coupled plasma mass spectrometry (ICP-MS) has been applied. The result reveals that 1 mol sample (C₅₆H₆₈N₈O₁₉Zn₃) can load 0.23 mol Cr³⁺ ions.

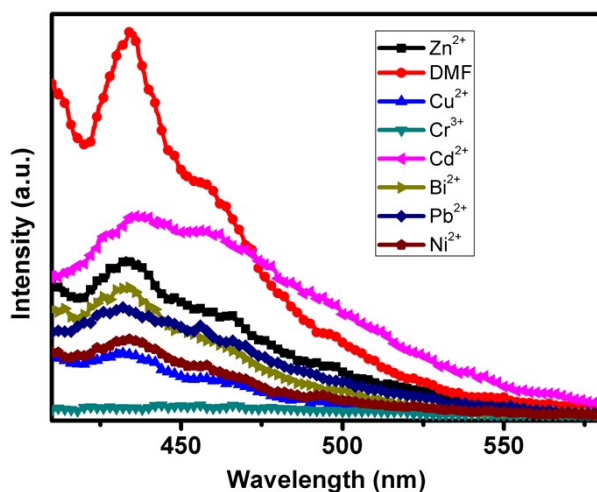


Fig. S10 The PL spectra of compound **1** incorporating different metal ions, activated in 5 mL DMF solution containing 0.01 M $M(\text{NO}_3)_x$.

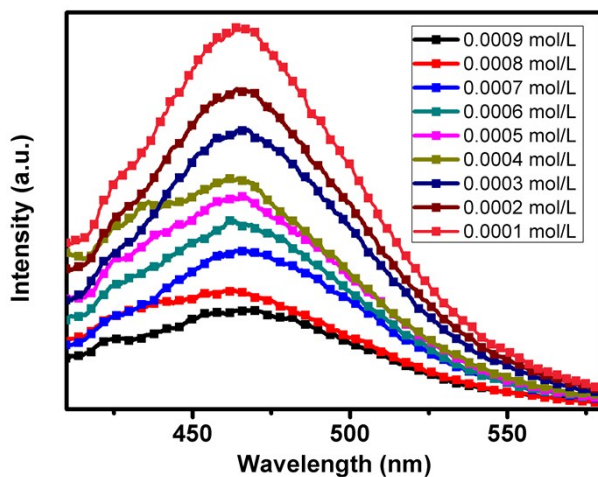


Fig. S11 The PL spectra of compound **1** in $\text{Cr}(\text{NO}_3)_3$ DMF solution at different concentrations.

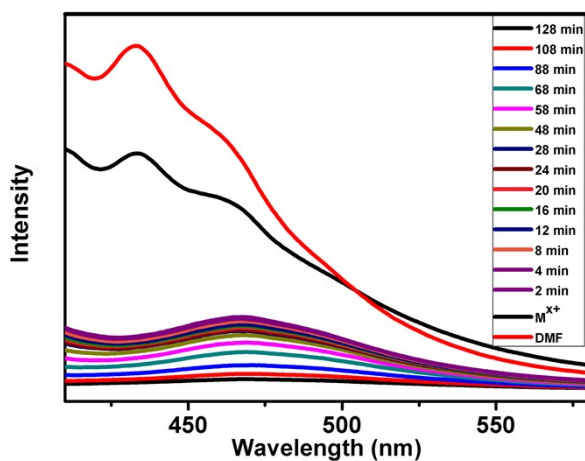


Fig. S12 Time-dependent photoluminescence intensities of $1\text{-}M^{x+}$ and $1\text{-}M^{x+} + \text{Cr}^{3+}$

($M^{x+} = Zn^{2+}, Bi^{2+}, Pb^{2+}$ and Cd^{2+}).

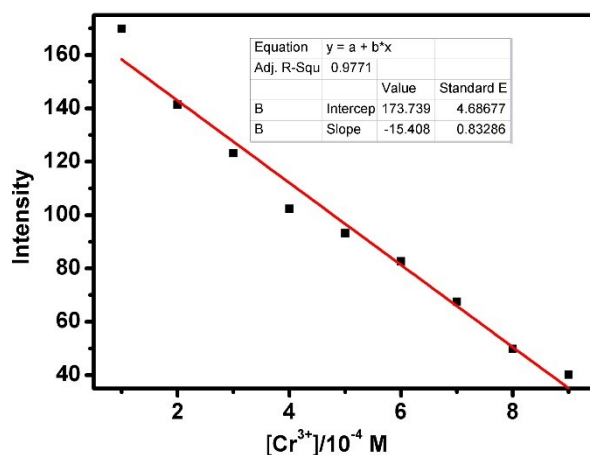


Fig. S13 Plot of the intensity for a mixture of **1**-Cr³⁺ in the range $1-9 \times 10^{-4}$ M.

The result of the analysis as follows:

Linear Equation: $Y = -15.41 \times X + 173.74$ $R = 0.9771$

$S = 15.41 \times 10^4$ $\delta = 1.17$ $K = 3.3$

$LOD = K \times \delta / S = 2.51 \times 10^{-5}$ M

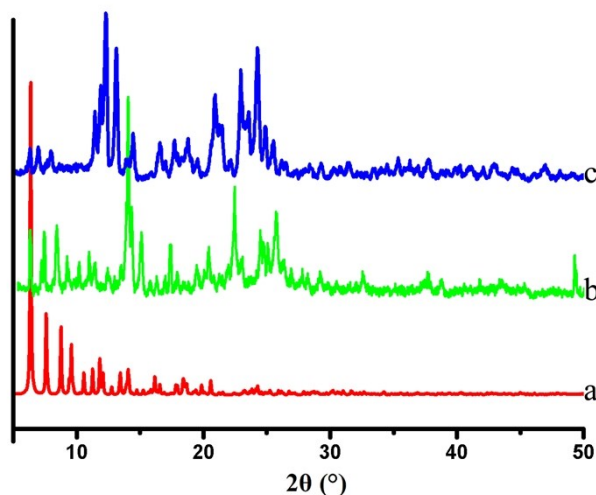


Fig. S14 Powder X-ray diffraction patterns of a) simulated from the X-ray single structure of **1**, b) as-synthesized **1**, and c) the sample incorporating Cr³⁺ ions.

The possible mechanism for quenching of the emission intensity:

Considering the channel diameter of compound **1**, it is possible for metal ions to

exist in the channel steadily. The carboxylic oxygen atoms and nitrogen atoms from the ligands inside of the channel can create a favorable coordination environment for metal ions. So the metal ions may bind to sites on the inner surface of the channels. The bonding of the metal ions to the organic ligands will change the energy level of the excited state of ligand, and results in a less efficient energy transition from the organic ligands to Zn^{2+} . For Cr^{3+} ions, the interactions between transition-metal ions and organic ligands quench the S1 state of organic ligands by d-d electron transfer of transition-metal ions, annihilating subsequent energy transfer.¹⁷⁻²⁰

References

1. F. M. Zhang, L. Z. Dong, J. S. Qin, W. Guan, J. Liu, S. L. Li, M. Lu, Y. Q. Lan, Z. M. Su and H. C. Zhou, *J. Am. Chem. Soc.*, 2017, **139**, 6183.
2. H. Wu, F. Yang, X. L. Lv, B. Wang, Y. Z. Zhang, M. J. Zhao and J. R. Li, *J. Mater. Chem. A*, 2017, **5**, 14525.
3. X. Liang, B. Li, M. Wang, J. Wang, R. Liu and G. Li, *ACS Appl. Mater. Interfaces*, 2017, **9**, 25082.
4. W. Phang, H. Jo, W. Lee, J. Song, K. Yoo, B. Kim and C. Hong, *Angew. Chem. Int. Ed.*, 2015, **5**, 5142.
5. D. N. Dybtsev, V. G. Ponomareva, S. B. Aliev, A. P. Chupakhin, M. R. Gallyamov, N. K. Moroz, B. A. Kolesov, K. A. Kovalenko, E. S. Shutova and V. P. Fedin, *ACS Appl. Mater. Interfaces*, 2014, **6**, 5161.
6. N. T. Nguyen, H. Furukawa, F. Gandara, C. A. Trickett, H. M. Jeong, K. E. Cordova, and O. M. Yaghi, *J. Am. Chem. Soc.*, 2015, **137**, 15394.
7. S. S. Nagarkar, S. M. Unni, A. Sharma, S. Kurungot and S. K. Ghosh, *Angew. Chem. Int. Ed.*, 2014, **53**, 2638.
8. P. Ramaswamy, N. E. Wong, B. S. Gelfand and G. K. Shimizu, *J. Am. Chem. Soc.*, 2015, **137**, 7640.
9. T.-N. Tu, N. Q. Phan, T.-T. Vu, H. L. Nguyen, K. E. Cordova and H. Furukawa, *J. Mater. Chem. A*, 2016, **4**, 3638.
10. W. J. Phang, W. R. Lee, K. Yoo, D. W. Ryu, B. Kim and C. S. Hong, *Angew. Chem. Int. Ed.*,

- 2014, **53**, 8383.
11. S. Kim, K. W. Dawson, B. S. Gelfand, J. M. Taylor and G. K. Shimizu, *J. Am. Chem. Soc.*, 2013, **135**, 963.
 12. S. Horike, W. Chen, T. Itakura, M. Inukai, D. Umeyama, H. Asakura and S. Kitagawa, *Chem. Commun.*, 2014, **50**, 10241.
 13. A. Karmakar, R. Illathvalappil, B. Anothumakkool, A. Sen, P. Samanta, A. V. Desai, S. Kurungot and S. K. Ghosh, *Angew. Chem. Int. Ed.*, 2016, **55**, 10667.
 14. V. G. Ponomareva, K. A. Kovalenko, A. P. Chupakhin, D. N. Dybtsev, E. S. Shutova and V. P. Fedin, *J. Am. Chem. Soc.*, 2012, **134**, 15640.
 15. V. G. Ponomareva, K. A. Kovalenko, A. P. Chupakhin, E. S. Shutova and V. P. Fedin, *Solid State Ionics*, 2012, **225**, 420.
 16. M. Sadakiyo, T. Yamada and H. Kitagawa, *J. Am. Chem. Soc.*, 2009, **131**, 9906.
 17. W. G. Lu, L. J. X. L. Feng and T. B. Lu, *Inorg. Chem.*, 2009, **48**, 6997.
 18. B. Zhao, H. L. Gao, X. Y. Chen, P. Cheng, W. Shi, D. Z. Liao, S. P. Yan and Z. H. Jiang, *Chem. Eur. J.*, 2006, **12**, 149.
 19. X. H. Zhou, L. Li, H. H. Li, A. Li, T. Yang and W. Huang, *Dalton Trans.*, 2013, **42**, 12403.
 20. Z. Chen, Y. W. Sun, L. L. Zhang, D. Sun, F. L. Liu, Q. G. Meng, R. M. Wang and D. F. Sun, *Chem. Commun.*, 2013, **49**, 11557.